mathematics

MDPI

Article

A Deep Learning Approach for Predicting Two-Dimensional Soil Consolidation Using Physics-Informed Neural Networks (PINN)

Yue Lu and Gang Mei *

School of Engineering and Technology, China University of Geosciences (Beijing), Beijing 100083, China
* Correspondence: gang.mei@cugb.edu.cn

Abstract: The unidirectional consolidation theory of soils is widely used in certain conditions and approximate calculations. The multidirectional theory of soil consolidation is more reasonable than the unidirectional theory in practical applications but is much more complicated in terms of index determination and solution. To address the above problem, in this paper, we propose a deep learning method using physics-informed neural networks (PINN) to predict the excess pore water pressure of two-dimensional soil consolidation. In the proposed method, (1) a fully connected neural network is constructed; (2) the computational domain, partial differential equation (PDE), and constraints are defined to generate data for model training; and (3) the PDE of two-dimensional soil consolidation and the model of the neural network are connected to reduce the loss of the model. The effectiveness of the proposed method is verified by comparison with the numerical solution of PDE for two-dimensional consolidation. Moreover, the FEM and the proposed PINN-based method are applied to predict the consolidation of foundation soils in a real case of Sichuan Railway in China, and the results are quite consistent. The proposed deep learning approach can be used to investigate large and complex multidirectional soil consolidation.

Keywords: engineering geology; soil consolidation; excess pore water pressure; deep learning; physics-informed neural network (PINN)

MSC: 35-04

check for updates

Citation: Lu, Y.; Mei, G. A Deep Learning Approach for Predicting Two-Dimensional Soil Consolidation Using Physics-Informed Neural Networks (PINN). *Mathematics* **2022**, *10*, 2949. https://doi.org/10.3390/math10162949

Academic Editors: Xiang Li, Shuo Zhang and Wei Zhang

Received: 5 July 2022
Accepted: 12 August 2022
Published: 16 August 2022

1. Introduction

Soil deformation and stability problems associated with soil consolidation occur during the construction of large infrastructures such as highways, embankments, and airports. Soil consolidation laws are complex and depend not only on the type and properties of the soil but also on its boundary conditions, drainage conditions, and types of loading [1,2]. Therefore, to ensure the safety of infrastructures, the study of multidirectional soil consolidation theory, which is closer to the actual working conditions, has broad application prospects and economic value.

There is much research work on soil consolidation. Terzaghi [3] in his seminal work on soil mechanics presented his consolidation theory for soil in 1925 as part of his comprehensive theory of soil mechanics. Biot [4] proposed his consolidation theory based on the effective stress principle, soil continuity, and equilibrium equation under the condition of considering the relationship between pore pressure and the soil skeleton deformation during soil consolidation. Schiffman [5] investigated the consolidation equation for the case of a linear increase in load with time and presented an analytical solution for one-dimensional soil consolidation under this situation. Indraratna [6] proposed a method for the radial consolidation of clays using a compression index and varying horizontal permeability.

Currently, most consolidation problems are analyzed using finite element analysis. The finite element method (FEM) is one of the most typical mesh-based numerical methods,

which is quite powerful and widely used in various science and engineering applications. However, when dealing with complex study areas or domains, the mesh generation in FEM is quite computationally expensive. Notably, in some cases, high-quality meshes cannot be achieved, thus leading to unsatisfactory computational accuracy [7,8]. Moreover, finite element analysis requires detailed material parameters of the study areas or domains. In some cases, detailed and accurate values of martial parameters are not easy to obtain.

Currently, there are two problems that occur when analyzing two-dimensional or three-dimensional soil consolidation. (1) The modeling process of traditional numerical methods is quite complicated for high-dimensional problems. (2) In general, traditional numerical methods are computationally quite inefficient when investigating multidimensional soil consolidation.

To address the above problems, in this paper, we propose a data-free deep learning method to predict two-dimensional soil consolidation using PINNs. In the proposed method, the prediction of excess pore water pressure is demonstrated for different boundary conditions: drainage at the top boundary and drainage at the top and bottom boundaries. First, we use DeepXDE [9], a library in Python, to define the computational domain, PDEs, constraints, and the number of training and testing data generated under these conditions for two-dimensional soil consolidation. Then, we construct the neural network. Finally, we connect the PDE of two-dimensional soil consolidation and the model of the neural network to reduce the loss of the model. Using this method, the excess pore water pressure of the soil can be predicted simply and efficiently.

A physics-informed neural network (PINN) is a type of neural network for solving PDEs using physical equations as operational constraints [10]. The idea behind a PINN is to convert physical constraints as additional loss functions in deep neural networks [11]. More details about the PINN will be introduced in Section 2.2.

The rest of this paper is organized as follows. Section 2 describes the details of this proposed method. Section 3 verifies this proposed method in two simple examples and analyses the results. In Section 4, the FEM and the proposed PINN-based method are applied to predict the consolidation of foundation soils in a real case of Sichuan Railway in China and make a comparative analysis. Section 5 discusses the advantages and shortcomings of the proposed deep learning method and points out future work. Finally, Section 6 concludes the paper.

2. Methods

2.1. Overview of the Proposed Deep Learning Method

In this paper, we propose a deep learning approach using PINN to predict the excess pore water pressure of two-dimensional soil consolidation (see Figure 1). First, we construct a fully connected neural network. Second, we define the PDE, time domain, and initial and boundary conditions for two-dimensional soil consolidation in DeepXDE, a Python library. Third, we connect the PDE to the neural network and tune the parameters to reduce the model loss. Finally, we employ the trained model to predict the excess pore water pressure. We verify this proposed method with two simple examples: two-dimensional consolidation for drainage at the top boundary and drainage at the top and bottom boundaries.

2.2. Background and Theory of PINN

In this section, we introduce how to employ PINN to solve the PDE.

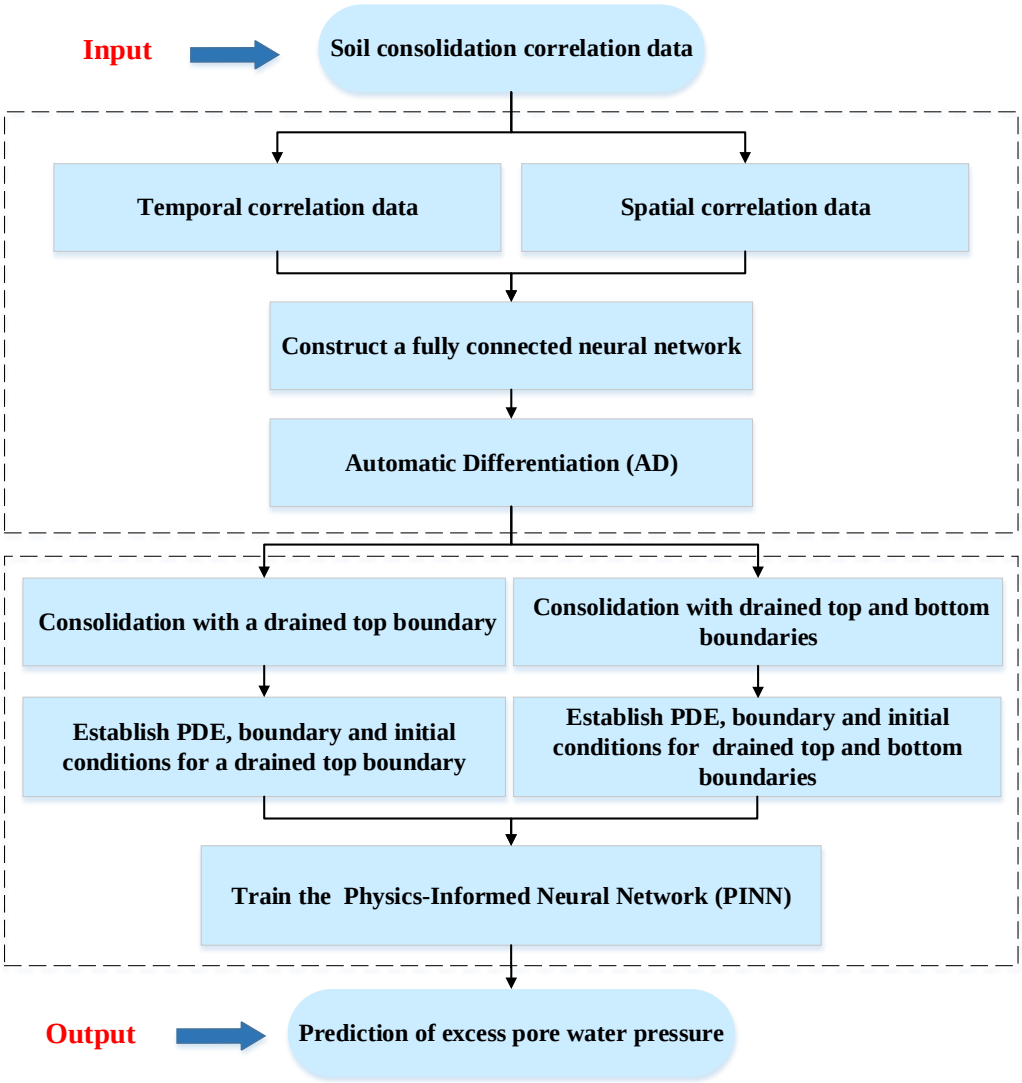

Figure 1. Flowchart of the proposed deep learning method.

2.2.1. Background of PINN

The idea of applying prior knowledge to deep learning was first proposed by Owhadi [12]. Subsequently, Raissi et al. [13,14] used Gaussian process regression to establish a representation of linear operator generalization to present uncertainty estimates for various physical problems, introducing and illustrating the PINN method for solving nonlinear PDEs [10]. Karniadakis et al. [15] proposed physics-informed machine learning as an algorithm that combines incomplete data with physical prior knowledge and discussed its various applications in forward and inverse problems.

Currently, PINNs have been increasingly used in various engineering problems, such as fluid mechanics [16–19]. For example, Bandai et al. [20] proposed the constitutive relation and soil water flux density for volumetric water content measurement based on a physical information neural network. Zhang, Z. [21] used a physics-informed neural network to simulate and predict the transient Darcy flow of unlabeled data in heterogeneous reservoirs. Bekele [22] used a PINN to solve forward and inverse problems of one-dimensional consolidation of soils.

2.2.2. Theory of PINN

A PINN combines PDEs and physics-informed constraints into the computation of a loss function to constrain the neural network and reduce the training loss, replacing

the actual observed data of the model, i.e., a "data-free" neural network. It approximates the PDE solution by training the neural network to minimize the loss function, including terms along the boundary of the space-time domain reflecting the initial and boundary conditions and residuals of PDEs at selected points in the domain. By combining values in the input domain with physical information, PINN generates an estimated solution to the point differential equation after training.

The process of solving the PDE requires the derivative of the input values. There are four methods for calculating derivatives: hand-coded, symbolic, numerical, and automatic. However, it is impractical to calculate the derivatives manually in the face of complex equations. The automatic differentiation (AD) used in a PINN uses exact expressions with floating-point values rather than symbolic strings, and there is no approximation error [23]. Undoubtedly, the prediction accuracy and efficiency are improved.

A PINN is composed of physical information, neural networks, and feedback mechanisms [24]. First, the physics-informed model is used to calculate the partial derivatives of the functions and to determine the loss of the equation terms. Then, the model is trained by connecting the two modular neural networks through a differentiation algorithm. Finally, continuous feedback adjustments are made to minimize the training losses. The PINN workflow schematic is illustrated in Figure 2.

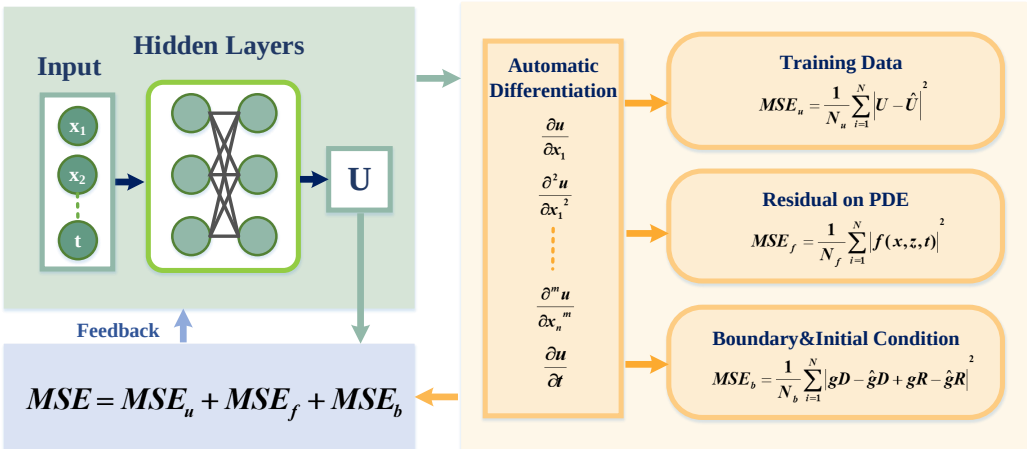

Figure 2. Illustration of a PINN algorithm for solving partial differential equations. This method uses AD technology to analyze and derive the integer derivative, and the obtained MSE is fed back to the neural network.

Physics-informed neural networks learn by minimizing the loss of the mean squared error. The mean square error formula of the neural network model is described in Equation (1) [10,25].

$$MSE = MSE_u + MES_f + MSE_b \tag{1}$$

where

$$MSE_u = \frac{1}{N_u}\sum_{i=1}^{N_u}|u(x,z,t) - \hat{u}(x,z,t)|^2 \tag{2}$$

$$MSE_f = \frac{1}{N_f}\sum_{i=1}^{N_f}|f(x,z,t)|^2 \tag{3}$$

$$MSE_b = \frac{1}{N_b}\sum_{i=1}^{N_b}|g_D(x,z,t) - \hat{g_D}(x,z,t) + g_R(x,z,t) - \hat{g_R}(x,z,t)|^2 \tag{4}$$

Here, (x,z,t) is the input to the training of a neural network model. In the proposed method, training points are randomly generated based on the physical constraints of the

governing PDE. $g_D(x, z, t)$ represents the initial training points, and $g_R(x, z, t)$ represents the boundary training points.

In this paper, we use the Python library DeepXDE to solve practical applications with PINNs. Solving differential equations with DeepXDE uses built-in modules to specify problems, including computational domains (geometry and time), PDEs, boundary/initial conditions, and neural network architecture [9]. The workflow of DeepXDE is shown in Figure 3. Furthermore, four boundary conditions (Dirichlet, Neumann, Robin, and periodic) are provided by this library. Initial conditions can be defined by IC modules. For example, the loss type, metric, optimizer, learning rate table, initialization, and regularization can be adjusted and selected by themselves according to different needs.

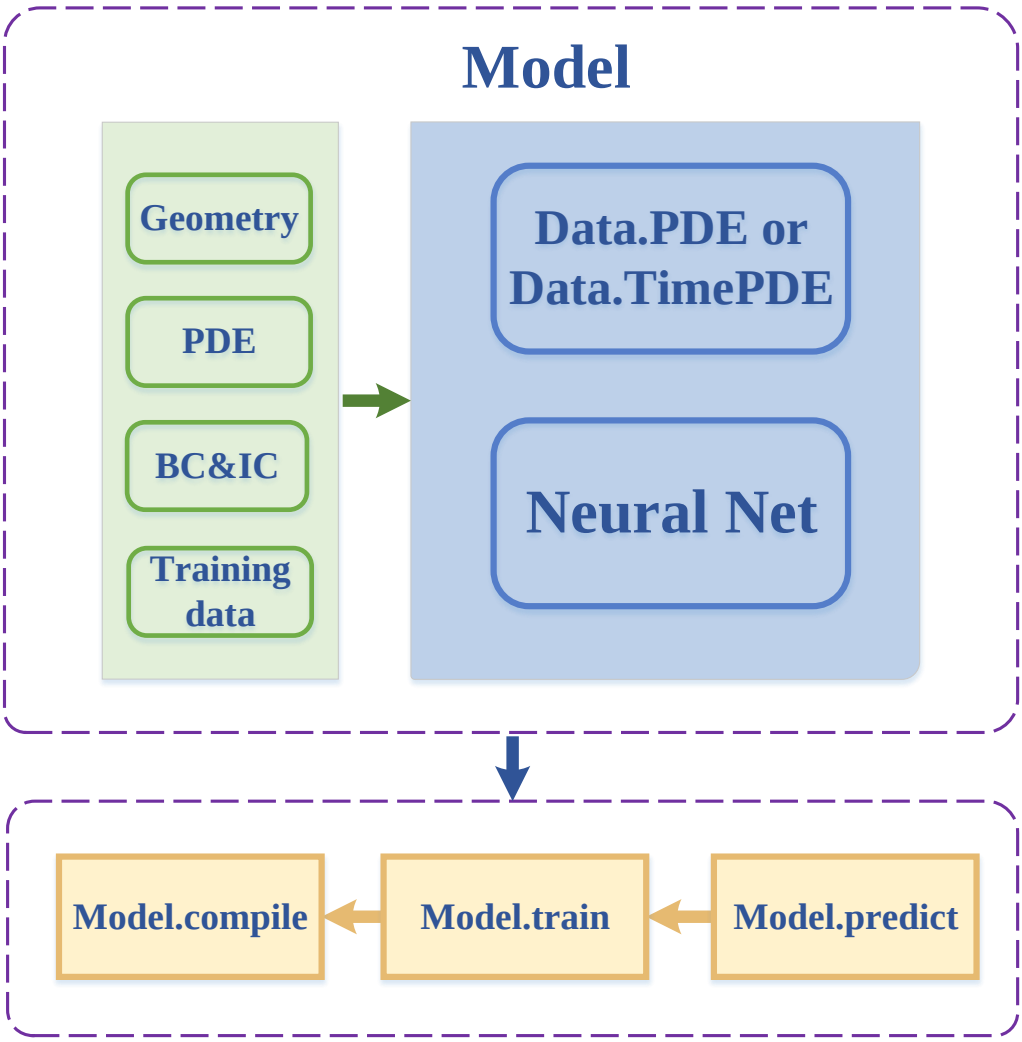

Figure 3. The workflow of DeepXDE. The green modules define the PDE and the training hyperparameters. The blue modules combine the PDE and training hyperparameters. The yellow modules are the three steps to solve the PDE.

2.3. Problem 1: Two-Dimensional Soil Consolidation for Drainage at Top Boundary

In this section, we introduce how to employ the deep learning approach to solve the problem of two-dimensional consolidation for drainage at a top boundary.

Rendulic [26] extended the one-dimensional consolidation theory to two or three dimensions and proposed the Terzaghi–Rendulic theory, assuming that the sum of normal stresses at any point in soil under constant external loads is a constant in consolidation. Therefore, the consolidation problem is the same as the thermal diffusion problem

of consolidation, and its mathematical expression is also called the diffusion equation (see Equation (5)).

$$\frac{\partial u}{\partial t} - C_v\left(\frac{\partial^2 u}{\partial x^2} + \frac{\partial^2 u}{\partial z^2}\right) = 0 \tag{5}$$

where u represents the excess pore water pressure, C_v represents the soil consolidation coefficient, and x and z represent the horizontal and vertical directions of the soil layer, respectively.

For two-dimensional consolidation of drainage at the top boundary, it is assumed that the bottom boundary is impervious. The excess pore water pressure dissipates only at the top boundary. The top boundary satisfies the Dirichlet boundary condition $u(x) = 0$, and the bottom boundary satisfies the Neumann boundary condition $\frac{\partial u}{\partial z} = 0$. A schematic diagram of consolidation for drainage at a top boundary is displayed in Figure 4. Assume that the initial excess pore water pressure distribution is q, and the initial excess pore pressure is uniformly distributed and equal to the surface overload. We set the thickness of the soil layer as H. The boundary conditions are mathematically expressed as Equation (6).

$$\begin{cases} u = 0 & (at\ \Gamma_b, t > 0) \\ \frac{\partial u}{\partial z} = 0 & (at\ \Gamma_t, t > 0) \\ u|_{x=|A|} = 0 & (t > 0) \end{cases} \tag{6}$$

In the proposed method, we use the PDE, boundary, and initial conditions of consolidation for drainage at a top boundary to generate training data, and then the trained model is applied to predict the excess pore water pressure.

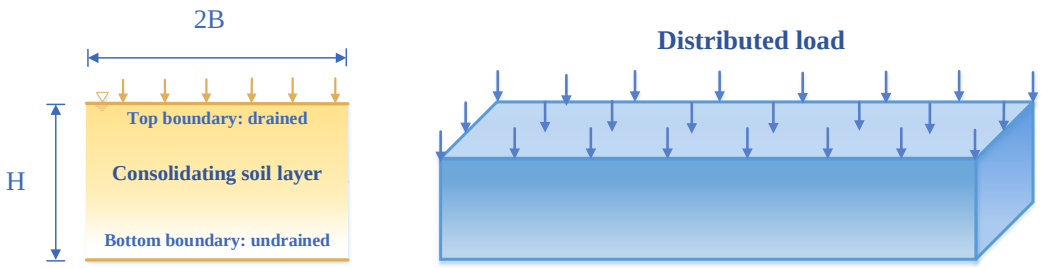

Figure 4. Schematic diagram of two-dimensional soil consolidation for drainage at a top boundary.

2.4. Problem 2: Two-Dimensional Soil Consolidation for Drainage at Top and Bottom Boundaries

In this section, we introduce how to employ the deep learning approach to solve the problem of two-dimensional soil consolidation for drainage at the top and bottom boundaries.

When both the top and bottom of the foundation are drainable boundaries, the excess pore water pressure is dissipated by both boundaries. The top and bottom boundaries satisfy the Dirichlet boundary condition $u(x) = 0$. A schematic diagram of consolidation drained at the top and bottom boundaries is displayed in Figure 5. Mathematically, this condition of soil consolidation for drainage at the top and bottom boundaries is expressed as Equation (7).

$$\begin{cases} u = 0 & (at\ \Gamma_t \cup \Gamma_b, t > 0) \\ u|_{x=|A|} = 0 & (t > 0) \end{cases} \tag{7}$$

Similarly, we set the initial excess pore pressure distribution as q. However, the maximum drainage distance for consolidation for drainage at the top and bottom boundaries is taken as half the thickness of the soil layer. Therefore, the thickness of the soil layer is set to double the drained thickness at the top boundary, i.e., 2H. We use the PDE, boundary, and initial conditions to generate training data, and then the trained model is applied to predict the excess pore water pressure.

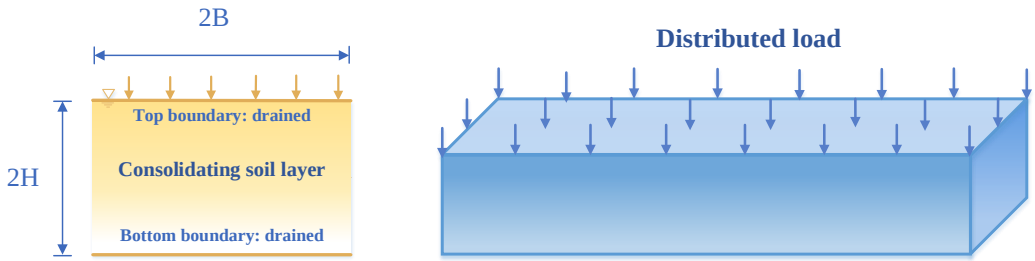

Figure 5. Schematic diagram of two-dimensional soil consolidation for drainage at the top and bottom boundaries.

3. Validation of the Proposed Deep Learning Approach

In this section, to verify the effectiveness of the proposed deep learning approach, we applied this proposed method with simple data to different boundary conditions and compared the results predicted by our approach with the numerical solutions obtained by the improved weighted residual method.

3.1. Experimental Environment

The experiments were conducted on a laptop with an NVIDIA GeForce RTX3070 laptop GPU and an AMD Ryzen 7 5800H with Radeon graphics. In order to obtain a better quantification of the machine, we tested the computer with CineBench R23, which resulted in a CPU (multi core) of 10920 and a CPU (single core) of 1392. The library used to implement the PINN was DeepXDE version 0.13.6.

3.2. Results of Consolidation with Drained Top Boundary

According to the weighted residual method, we assumed that there is drainage sand well at the center of the substrate (load) and considered its influence range in the horizontal direction to be limited, which is shown by the numerical analysis as $A = 2B$. Since there is usually no drainage sand well at the center of the load in actual projects, the numerical solution was obtained after excluding this condition (Equation (8)).

$$u = \frac{16q}{\pi^2} \sum_{m=1,3,5\ldots}^{\infty} \frac{1}{m^2} \sin\left(\frac{\pi m}{2A}(x+A)\right) \sin\left(\frac{\pi m}{2H} Z\right) e^{-\left(\frac{1}{A}+\frac{1}{4H^2}\right)^2 C_v m^2 \pi^2 t} \tag{8}$$

For a numerical example of a drained top boundary, we set the soil layer thickness to $H = 1$ m, and the soil consolidation coefficient was $C_v = 0.01$ cm^2/s. In addition, we assumed that the foundation was subjected to a distributed load $q = 10$ kN/m^2 and that the load level affects the range $A = 1$ m. The numerical solution Equation (8) was used as the reference solution for the training results. The geometry module of this example was Rectangle [−1,0] [1,1]. Soil consolidation is a time-dependent PDE problem, and the time domain calculated in this experiment ranged from 0 to 1. Finally, the input of the PDE system and the construction of the physical information model were completed. The residuals were tested by sampling 100 points in the domain, initial and boundary conditions and using 1000 points to test the PDE residuals.

Here, we used a fully connected neural network of depth 6 (i.e., 5 hidden layers) and width 32. Temporal and spatial partial derivatives of excess pore water pressure were determined by AD in this neural network. Values of (x, z, t) were used as the input of the neural network, where this model predicts the excess pore water pressure as the output. The Adam optimizer was chosen to train 10,000 epochs for this experiment, and the time required was approximately 15 s. The time spent on model training was proportional to the number of hidden units, hidden layers, and training epochs, and we tuned the parameters depending on the desired accuracy.

On the established soil consolidation for the drained top boundary model, 100 points were randomly selected, the numerical solution and the predictive solution were entered,

and the color maps of the numerical solution and the predictive solution at different times were obtained by interpolation, as shown in Figure 6.

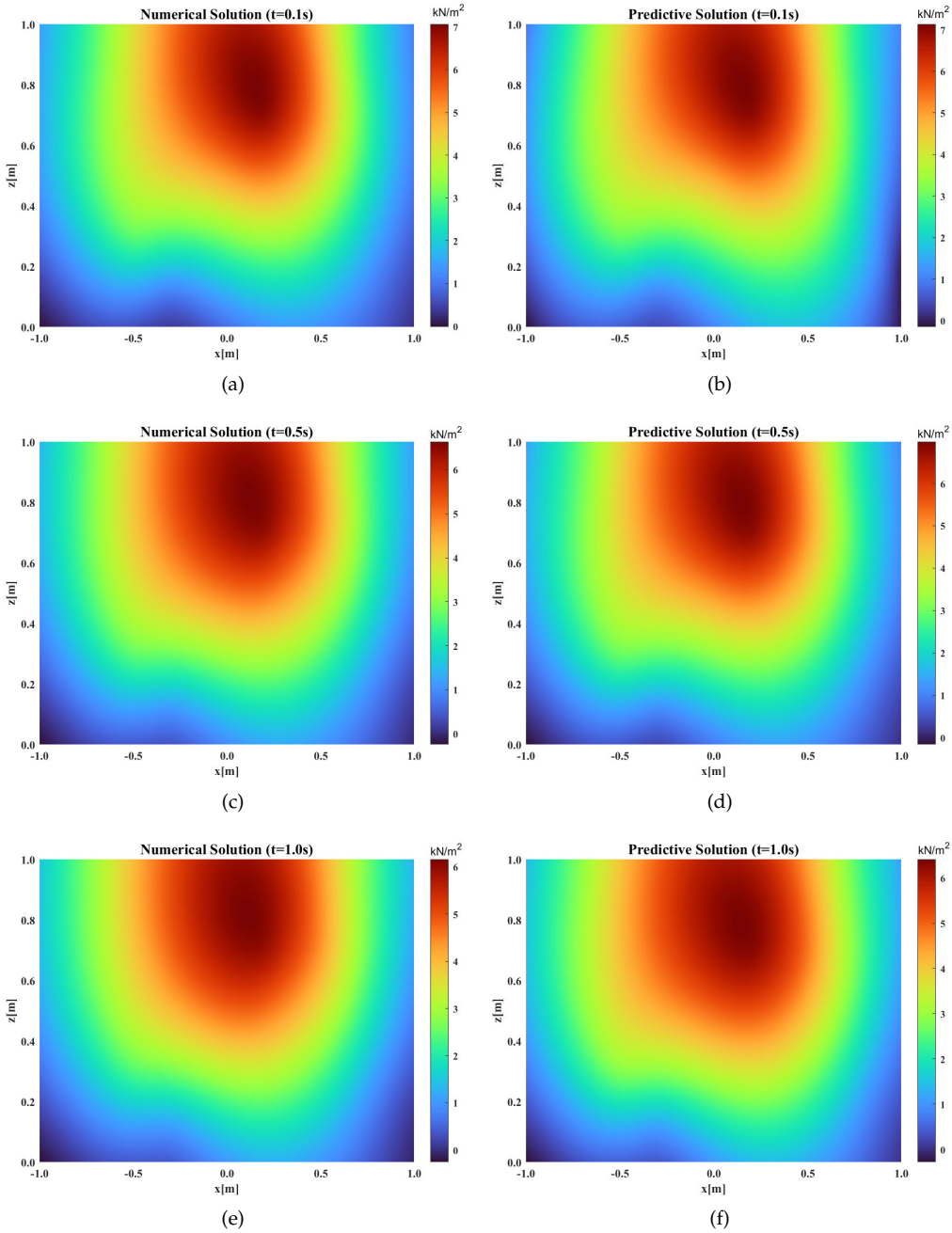

Figure 6. Color maps for numerical solution and predicted solution of two-dimensional soil consolidation for drainage at a top boundary at different times. (**a**) Numerical solution (t = 0.1 s); (**b**) Predictive solution (t = 0.1 s); (**c**) Numerical solution (t = 0.5 s); (**d**) Predictive solution (t = 0.5 s); (**e**) Numerical solution (t = 1.0 s); (**f**) Predictive solution (t = 1.0 s).

The color maps of the numerical solution and the predictive solution of consolidation with drained top boundary are illustrated in Figure 6. We can observe the excellent consistency between the numerical solution and the predictive solution at different times. The excess pore water pressure is at its maximum at the intersection of the load center and the bottom of the soil layer and dissipates gradually with time.

The final train loss and test loss of this two-dimensional soil consolidation for drainage in the top boundary model are displayed in Figures 7 and 8.

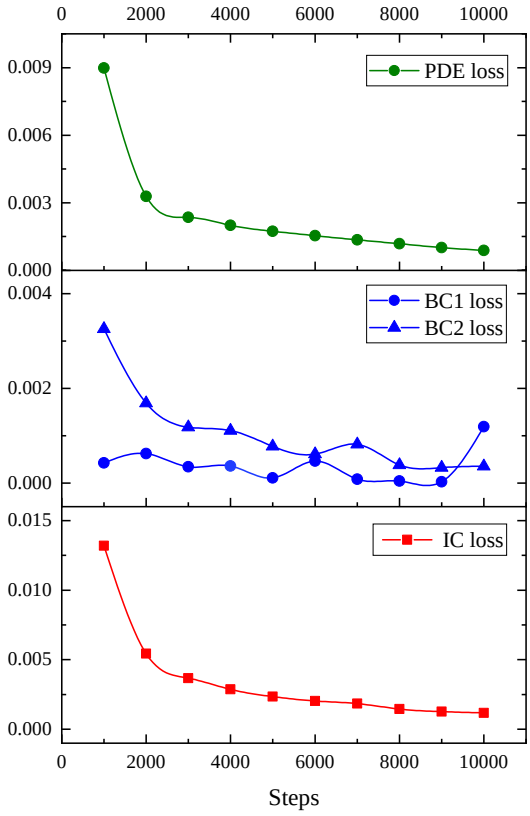

Figure 7. Training results for two-dimensional consolidation model of drainage at a top boundary.

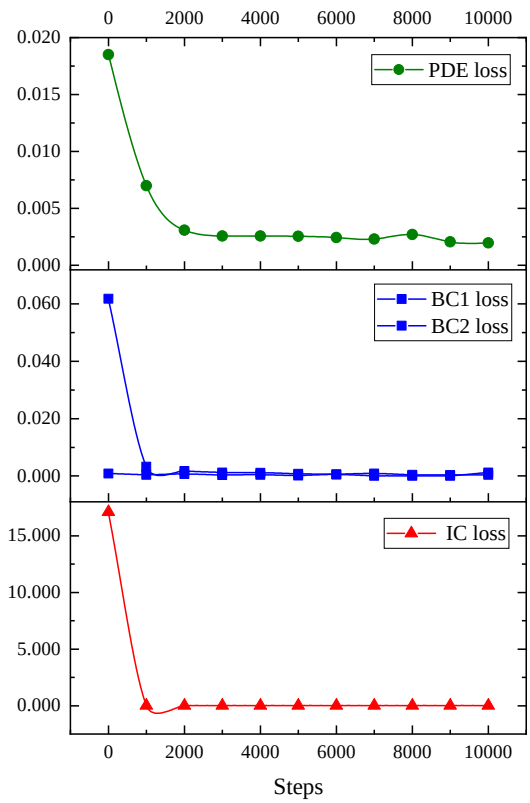

Figure 8. Testing results for two-dimensional consolidation model of drainage at a top boundary.

According to Figures 7 and 8, it is observed that the loss of PDE, boundary, and initial conditions of this model in training and testing has a good downward trend and gradually tends to be stable after 2000 epochs of training.

The test measure in this experiment is the ratio of training loss to the numerical solution, which better reflects the training results of the model (see Equation (9)). The final mean squared error loss and test metric of a drained top boundary model with two-dimensional consolidation are displayed in Figure 9.

$$test\ metric = \frac{u - \hat{u}}{u} \tag{9}$$

In this case, the training loss drops to 2.64×10^{-3}, the test loss drops to 3.67×10^{-3}, and the test metric drops to 6.82×10^{-2}.

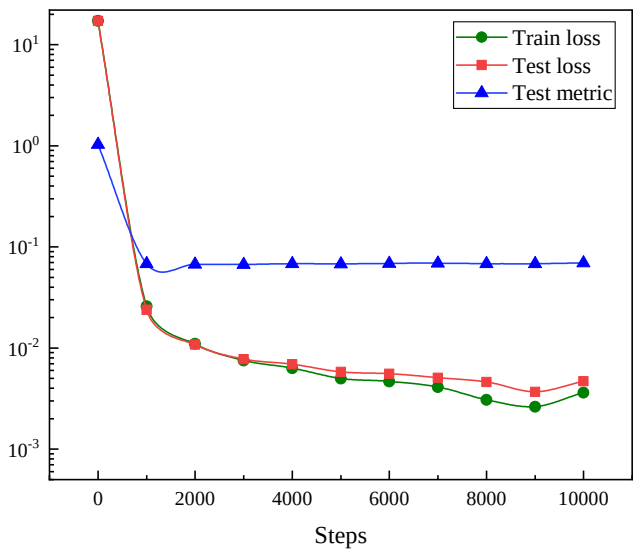

Figure 9. Mean squared error loss and test metric for two-dimensional consolidation model of drainage at a top boundary.

3.3. Results of Consolidation for Drained Top and Bottom Boundaries

For two-dimensional consolidation drained at the top and bottom boundaries, we contemplated using the same neural network model as described in Section 3.2. However, the excess pore water pressure in this condition was permitted to dissipate through both boundaries, corresponding to the absence of pore water in the center of the soil layer. For comparison, we set the soil layer thickness to 2H = 2 m, and the geometry module of this example was Rectangle [−1,0] [1,2]. The other constraints were the same as those in Section 3.2.

Similarly, we used a fully connected neural network of depth 6 (i.e., 5 hidden layers) and width 32. The temporal and spatial partial derivatives of excess pore water pressure were determined by AD in this neural network. Values of (x, z, t) were used as the input of the neural network, where this model predicts the excess pore water pressure as the output. The Adam optimizer was chosen to train 10,000 epochs for this experiment. Since the boundary constraints of double-sided drainage are simpler than those of single-sided drainage, the training time of the model was shorter.

On the established soil consolidation for the drainage at the top and bottom boundary models, 100 points were randomly selected, the numerical solution and the predictive solution were entered, and the color maps of the numerical solution and the predictive solution at different times were obtained by interpolation, as displayed in Figure 10.

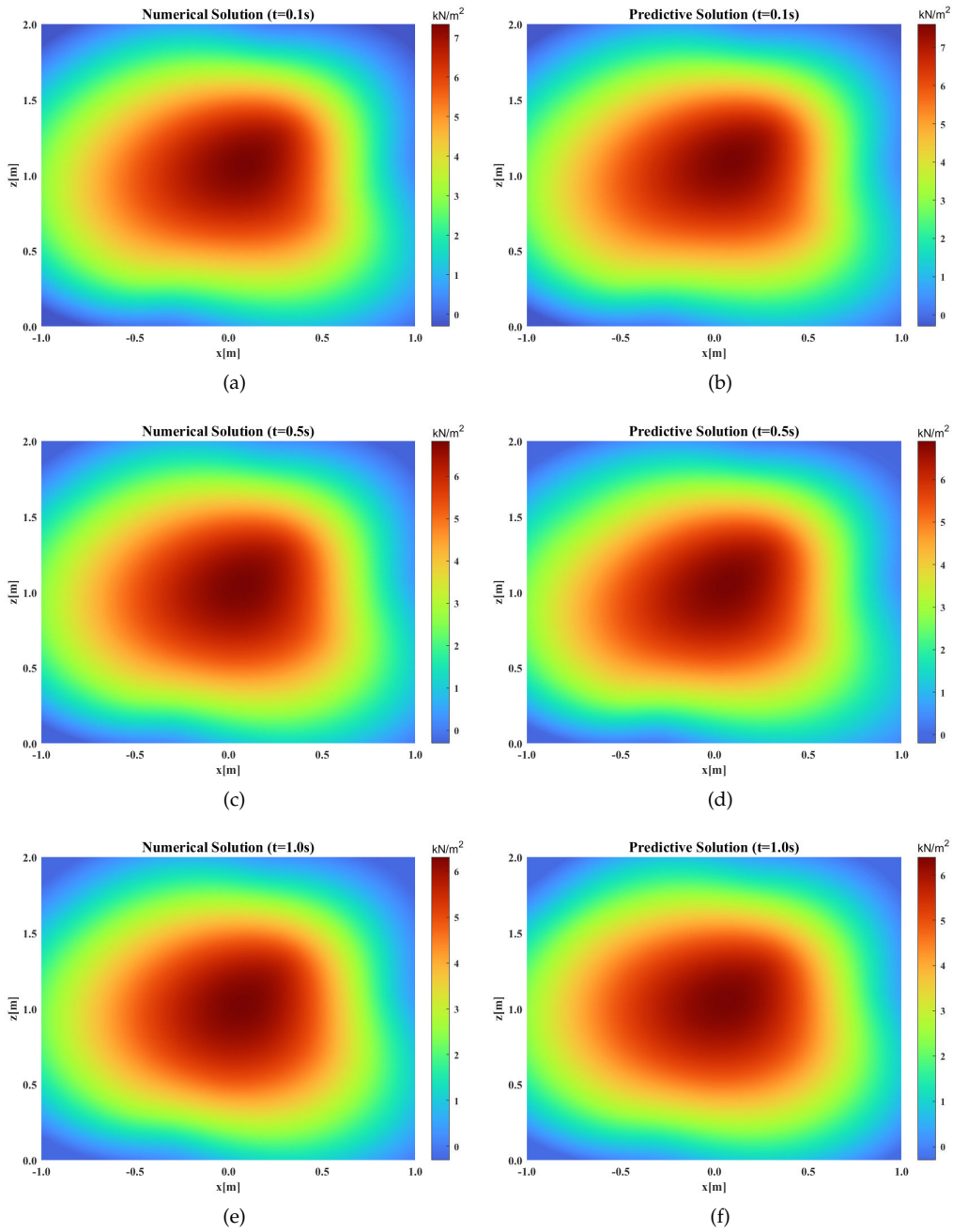

Figure 10. Color maps for numerical solution and predicted solution of two-dimensional soil consolidation for drainage at the top and bottom boundaries at different times. (**a**) Numerical solution (t = 0.1 s); (**b**) Predictive solution (t = 0.1 s); (**c**) Numerical solution (t = 0.5 s); (**d**) Predictive solution (t = 0.5 s); (**e**) Numerical solution (t = 1.0 s); (**f**) Predictive solution (t = 1.0 s).

The color maps of the numerical solution and the predictive solution of consolidation with drained top and bottom boundaries are illustrated in Figure 10. We can observe the excellent consistency between the numerical solution and the predictive solution at different times. The excess pore water pressure is at its maximum at the intersection of the load center and the middle of the soil layer and dissipates gradually with time.

The final train loss and test loss of this two-dimensional soil consolidation for drained at the top and bottom boundary models are displayed in Figures 11 and 12.

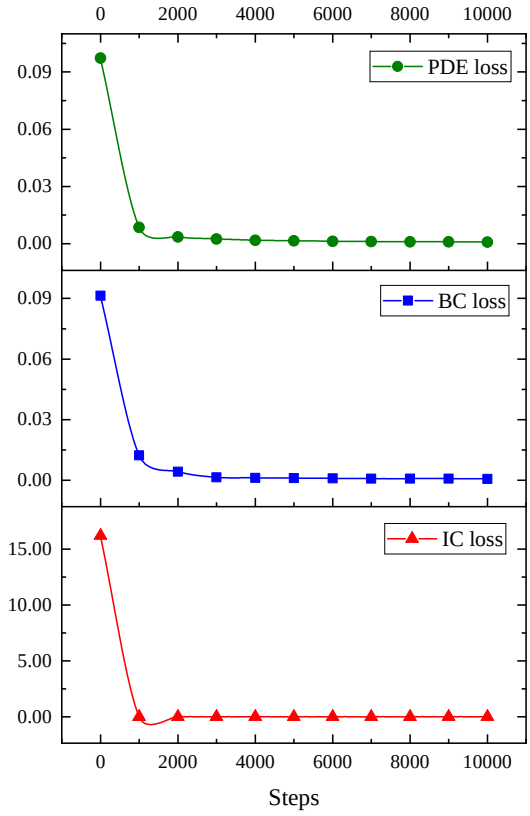

Figure 11. Training results for two-dimensional consolidation model of drainage at the top and bottom boundaries.

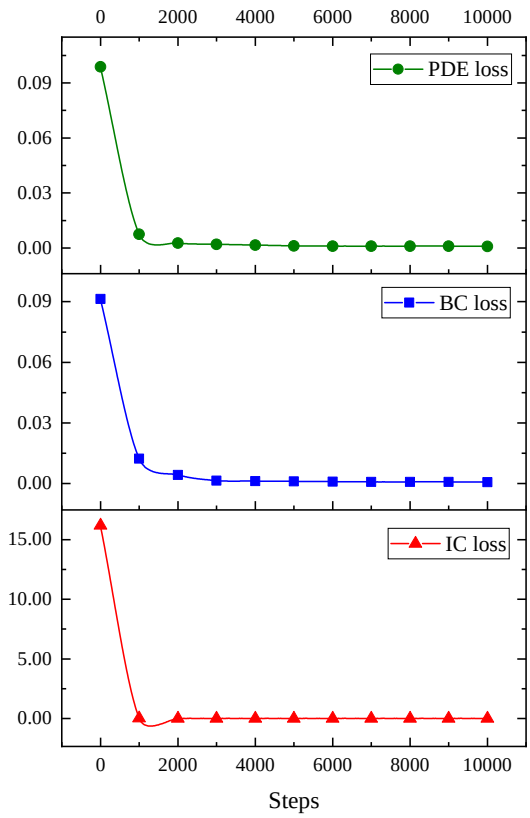

Figure 12. Testing results for two-dimensional consolidation model of drainage at the top and bottom boundaries.

According to Figures 11 and 12, it is observed that the loss of PDE, boundary, and initial conditions of this model in training and testing have a good downward trend and gradually tend to be stable after 2000 epochs of training.

The final mean squared error loss and test metric of two-dimensional consolidation for drainage at the top and bottom boundaries are displayed in Figure 13.

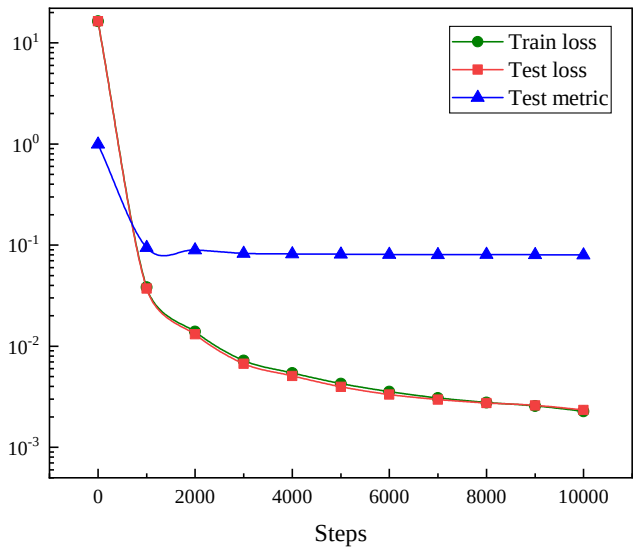

Figure 13. Mean squared error loss and test metric for two-dimensional consolidation model of drainage at the top and bottom boundaries.

In this case, the training loss drops to 2.27×10^{-3}, the test loss drops to 2.34×10^{-3}, and the test metric drops to 7.96×10^{-2}. We observed the great performance of the PINN models in predicting excess pore water pressure.

4. Application of the Proposed Deep Learning Approach

In this section, the proposed deep learning approach was used to predict the excess pore water pressure of soil layers in a real case. Details of the application are introduced as follows.

4.1. Engineering Background

The case we studied was a railway subgrade. The railway runs from Chengdu West Station to Pujiang Station, passing through the Sichuan Basin, the western part of the Sichuan Plain, and the hilly edge of the basin, with an altitude of 500~600 m. We selected one section of the railway. The length of this line is 182.6 m in the territory of Dayi D3K51 + 901 ~ D3K52 + 083.6 m section. For the parameters of the soil, see Table 1.

Table 1. Parameters of the soil.

Parameter	γ_{unsat} (kN/m^3)	γ_{sat} (kN/m^3)	k_x (m/day)	k_y (m/day)	E (kN/m^2)	c (kN/m^2)	φ (°)	ψ (°)	μ
Clay	15	18	1×10^{-4}	1×10^{-4}	1000	2	24	0	0.33
Peat	8	11	2×10^{-3}	2×10^{-3}	350	5	20	0	0.35
Sand	16	20	1	1	3000	1	30	0	0.30

The shape of the subgrade was trapezoidal, filled with sand, with a width of 16 m and a height of 4 m. The soil layers were peat and clay layers. For the geological profile of the subgrade, see Figure 14.

The layered construction scheme was used in this case study area. Stage 1 involved filling 2 m of the embankment and then consolidating the soil layers for 200 days. Stage

2 involved filling 2 m of the embankment, and the soil layers will be consolidated for a long time.

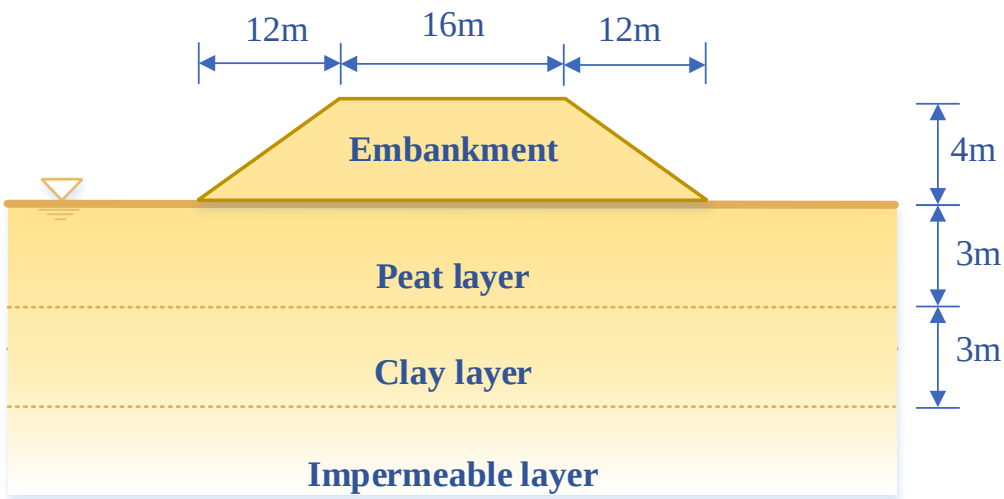

Figure 14. Schematic diagram of geological section of the subgrade.

4.2. Results of Finite Element Analysis

To further verify the accuracy of the PINN results, PLAXIS software (https://www.bentley.com/en/products/brands/plaxis, accessed on 1 August 2022) was used to numerically investigate the above engineering problems. The Mohr–Coulomb model was used in PLAXIS. Due to the symmetry of the geometric model, the right half of the model was intercepted for analysis. The plane strain model was selected and analyzed. The boundary conditions are defined by standard fixed boundaries in the PLAXIS. The consolidation control standard for this case is maximum excess pore water of less than 1 kN/m^2.

By selecting a point in the middle of the soft soil layer near the left boundary to reflect the development of excess pore water pressure under the subgrade during the construction of the subgrade, the change process of excess pore water pressure is illustrated in Figure 15. It can be observed that the excess pore water pressure rises rapidly with the filling of the subgrade and decreases gradually with time during the consolidation period. It takes approximately 650 days from the start of stage 1 to the complete consolidation of the soil layers of the subgrade. The distribution of excess pore water pressure at 650 days is illustrated in Figure 16. It can be observed that the excess pore water pressure under the center of the subgrade is maximum and less than 1 kN/m^2.

4.3. Results of PINN-Based Method

In this section, the proposed PINN approach was employed to predict the excess pore water pressure of the subgrade in this case study area. The bottom of the foundation was the impervious layer. This model was constructed in the same way as described in Section 2.3.

The load covered the range A = 20 m, and the thickness of the foundation soil layer was H = 6 m. Therefore, the geometry module of the case study area was a Rectangle [0,−6] [20,0]. Two different prediction models were developed based on the consolidation coefficients of different soil layers. The residuals were tested by sampling 1000 points in the domain, initial and boundary conditions and using 1000 points to test the PDE residuals. Similarly, a fully connected neural network of depth 6 (i.e., 5 hidden layers) and width 32 was used. The Adam optimizer was chosen to train 50,000 epochs for this experiment.

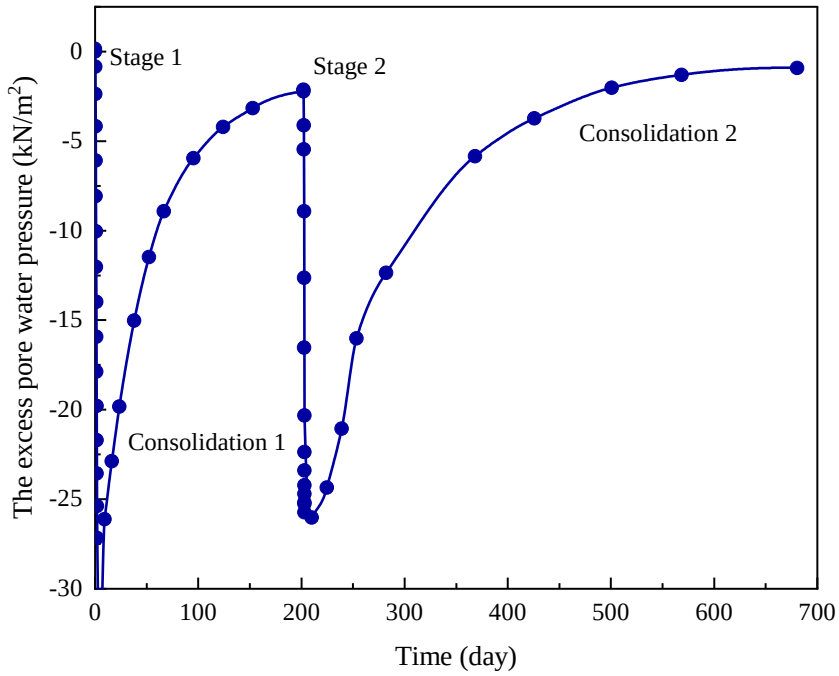

Figure 15. Line chart of excess water pressure change process during consolidation.

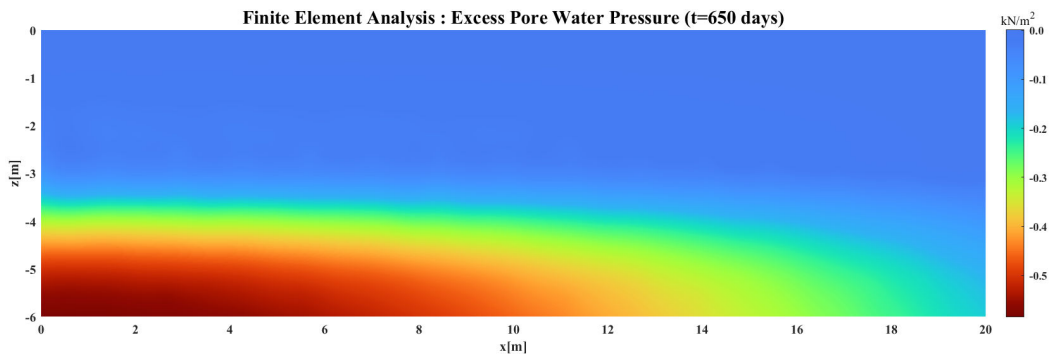

Figure 16. Color map of excess pore water pressure based on the finite element analysis.

After the training of the constructed model above, the excess pore water pressure in the soil reaches a desirable value at approximately 650 days. The distribution of excess pore water pressure at 650 days is illustrated in Figure 17.

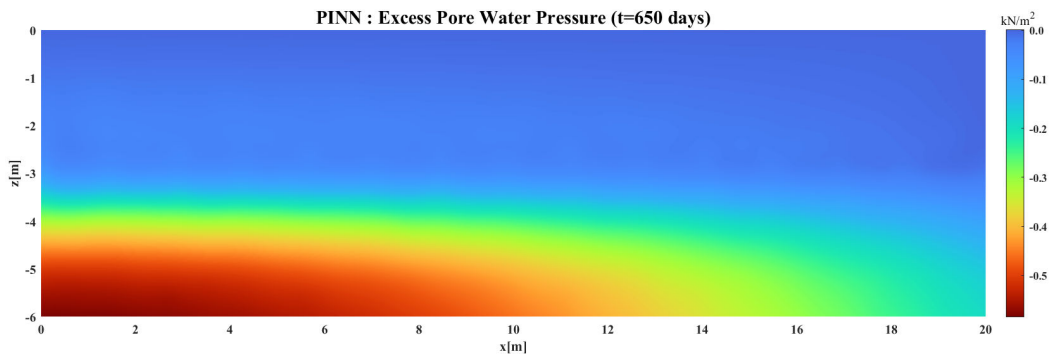

Figure 17. Color map of excess pore water pressure based on the proposed PINN-based method.

4.4. Comparative Analysis

As illustrated in Figure 15, it was obtained that the consolidation control standard was achieved after 600 days, and for comparison, the excess pore water pressure distribution

within the soil layer at 650 days was plotted separately using two methods (i.e., the FEM and the proposed PINN-based method).

The results obtained from the finite element analysis and the PINN-based method are shown in Figures 16 and 17. The color plots are obtained by interpolation of the nearest excess pore pressure values from the actual grid points and are chosen here only for visualization.

Under the same conditions, the excess pore water pressure prediction by FEM and the PINN-based method was compared, and the results were quite consistent. The consistency between the FEM results and the PINN-based results indicates that the deep learning model reasonably predicts the excess pore pressure based on the initial and boundary training data alone. Moreover, the PINN-based method does not require generating meshes, and it does require fewer detailed material parameters of the study area or domain than that of the FEM. Therefore, using this method, the excess pore water pressure of the soil can be predicted simply and efficiently. This demonstrates the remarkable accuracy of the physical constraints and the potential of the PINN-based method applied to numerically investigate the geotechnical consolidation under more complex conditions.

5. Discussion

5.1. Advantages of the Proposed Method

There are two advantages of the proposed deep learning approach.

(1) Compared with traditional methods, the proposed method is computationally simple. In the proposed PINN method, the physical information including partial differential equations, initial conditions, and boundary conditions of soil consolidation is defined without having actual data, and the data in the computational domain are randomly and automatically generated for model training.
(2) Compared with traditional methods, the proposed method is computationally efficient. In the proposed PINN method, defined physical information is loosely coupled. The prediction of excess pore water pressure in two-dimensional soil consolidation can be adjusted and is highly adaptable to consolidation problems in different engineering environments without the need for remodeling.

5.2. Shortcomings of the Proposed Method

The proposed method is proposed based on PINN. PINN has good performance in solving two-dimensional soil consolidation, but complex high-dimensional PDEs usually have no precise solutions, and there is no completely accurate reference value to judge the training accuracy of the PINN training model. In addition, for complex engineering problems, stronger boundary conditions are needed to improve the fit to the engineering problems. Therefore, for some high-dimensional problems with weak boundary conditions, deep neural networks, as a general function approximator, can only obtain an approximate solution to the problem by minimizing the loss of the training model. How to further improve the computational accuracy is the current problem with PINN.

5.3. Outlook and Future Work

In future work, we will consider various constraints to improve the training accuracy of the neural network as much as possible and assess the applicability of this proposed deep learning approach using PINN to other engineering geology problems.

There are several strategies to improve the accuracy of neural network model training results. Adding more data is a good idea for ordinary models, but this idea does not apply to complex geological engineering problems with a lack of observation data. At present, the most effective method for PINN is algorithm optimization. It is well understood that deep learning algorithms are driven by parameters that mainly affect the learning process results. In the future, we plan to combine several algorithms to build high-precision models. However, the choice of algorithm is difficult, and this intuition comes from experience and

practice. Therefore, all relevant models should be applied, and comparative performance should be checked.

The advantage of PINN in solving geotechnical problems is the use of prior knowledge and logic to discover the characteristics of the problem, but it lacks the ease of consistency with real data [27]. Further research is needed to achieve a perfect combination of physical knowledge and neural networks. Many improvements to the methods currently proposed are still possible, and some theoretical problems remain unresolved. There is still potential for development in optimizing training PINNs and expanding PINNs to solve multiple equations.

We present a simple PINN problem for predicting the excess pore water pressure of two-dimensional consolidation, but this method can be extended to many large and complex multidirectional soil consolidation problems. The combination of deep learning models and physical laws is a new trend in the development of engineering geology, which is still in the initial stage of research and has not yet been widely applied to practical engineering. In the future, such as in foundation deformation monitoring of large facilities, the monitoring and early warning of landslides can be attempted using the proposed deep learning method.

6. Conclusions

In this paper, we propose a deep learning method using a PINN to predict the excess pore water pressure of two-dimensional soil consolidation. The essential idea behind the proposed method is to implement data-free model training with physics-informed constrained neural networks. In the proposed method, we present two simple examples of how to predict soil excess pore water pressure with different boundary conditions. In the proposed method, (1) a fully connected neural network is constructed, (2) the computational domain, partial differential equation (PDE), and constraints are defined to generate data for model training, and (3) the PDE of two-dimensional soil consolidation and the model of the neural network is connected to reduce the loss of the model. The effectiveness of the method is verified by comparing it with the numerical solution of the PDE for two-dimensional consolidation. Moreover, the excess pore water pressure prediction by FEM and the PINN- based method is compared, and the results are quite consistent. The consistency between the FEM results and the PINN-based results indicates that the deep learning model reasonably predicts the excess pore pressure based on the initial and boundary training data alone. In the future, the proposed deep learning approach can be used to investigate large and complex multi-directional soil consolidation.

Author Contributions: Conceptualization, Y.L. and G.M.; methodology, Y.L. and G.M.; software, Y.L. and G.M.; validation, Y.L. and G.M.; formal analysis, Y.L. and G.M.; investigation, Y.L. and G.M.; resources, Y.L. and G.M.; data curation, Y.L. and G.M.; writing—original draft preparation, Y.L.; writing—review and editing, Y.L. and G.M.; visualization Y.L. and G.M.; supervision, G.M.; project administration, G.M.; funding acquisition, G.M. All authors have read and agreed to the published version of the manuscript.

Funding: This research was jointly supported by the National Natural Science Foundation of China (Grant Nos. 11602235), and the Major Program of Science and Technology of Xinjiang Production and Construction Corps (2020AA002). The authors would like to thank the editor and the reviewers for their helpful comments and suggestions.

Institutional Review Board Statement: Not applicable.

Informed Consent Statement: Not applicable.

Data Availability Statement: Not applicable.

Acknowledgments: The authors would like to thank the editor and the anonymous reviewers for their valuable comments.

Conflicts of Interest: The authors declare no conflict of interest.

References

1. Lo, W.C.; Sposito, G.; Lee, J.W.; Chu, H. One-dimensional consolidation in unsaturated soils under cyclic loading. *Adv. Water Resour.* **2016**, *91*, 122–137. [CrossRef]
2. Pham, B.T.; Nguyen, M.D.; Bui, K.T.T.; Prakash, I.; Chapi, K.; Bui, D.T. A novel artificial intelligence approach based on Multi-layer Perceptron Neural Network and Biogeography-based Optimization for predicting coefficient of consolidation of soil. *Catena* **2019**, *173*, 302–311. [CrossRef]
3. Terzaghi, K. *Erdbaumechanik auf Bodenphysikalischer Grundlage*; Deuticke: Leipzig, Germany, 1925.
4. Biot, M.A. General Theory of Three-Dimensional Consolidation. *J. Appl. Phys.* **1941**, *12*, 155–164. [CrossRef]
5. Schiffman, R.L.; Stein, J.R. One-Dimensional Consolidation of Layered Systems. *J. Soil Mech. Found. Div.* **1970**, *96*, 1499–1504. [CrossRef]
6. Indraratna, B.; Rujikiatkamjorn, C.; Sathananthan, I. Radial consolidation of clay using compressibility indices and varying horizontal permeability. *Can. Geotech. J.* **2005**, *42*, 1330–1341. [CrossRef]
7. Ng, A.K.L.; Small, J.C. Use of coupled finite element analysis in unsaturated soil problems. *Int. J. Numer. Anal. Methods Geomech.* **2000**, *24*, 73–94. [CrossRef]
8. Yarushina, V.M.; Podladchikov, Y.Y. (De)compaction of porous viscoelastoplastic media: Model formulation. *J. Geophys. Res. Solid Earth* **2015**, *120*, 4146–4170. [CrossRef]
9. Lu, L.; Meng, X.; Mao, Z.; Karniadakis, G.E. DeepXDE: A Deep Learning Library for Solving Differential Equations. *SIAM Rev.* **2021**, *63*, 208–228. [CrossRef]
10. Raissi, M.; Perdikaris, P.; Karniadakis, G.E. Physics-informed neural networks: A deep learning framework for solving forward and inverse problems involving nonlinear partial differential equations. *J. Comput. Phys.* **2019**, *378*, 686–707. [CrossRef]
11. Blechschmidt, J.; Ernst, O.G. Three ways to solve partial differential equations with neural networks—A review. *GAMM-Mitteilungen* **2021**, *44*, e202100006. [CrossRef]
12. Owhadi, H. Bayesian Numerical Homogenization. *Multiscale Model. Simul.* **2015**, *13*, 812–828. [CrossRef]
13. Raissi, M.; Perdikaris, P.; Karniadakis, G.E. Inferring solutions of differential equations using noisy multi-fidelity data. *J. Comput. Phys.* **2017**, *335*, 736–746. [CrossRef]
14. Raissi, M.; Perdikaris, P.; Karniadakis, G.E. Machine learning of linear differential equations using Gaussian processes. *J. Comput. Phys.* **2017**, *348*, 683–693. [CrossRef]
15. Karniadakis, G.E.; Kevrekidis, I.G.; Lu, L.; Perdikaris, P.; Wang, S.; Yang, L. Physics-informed machine learning. *Nat. Rev. Phys.* **2021**, *3*, 422–440. [CrossRef]
16. Raissi, M.; Yazdani, A.; Karniadakis, G.E. Hidden fluid mechanics: Learning velocity and pressure fields from flow visualizations. *Science* **2020**, *367*, 1026–1030. [CrossRef] [PubMed]
17. Tartakovsky, A.M.; Marrero, C.O.; Perdikaris, P.; Tartakovsky, G.D.; Barajas-Solano, D. Physics-Informed Deep Neural Networks for Learning Parameters and Constitutive Relationships in Subsurface Flow Problems. *Water Resour. Res.* **2020**, *56*, e2019WR026731. [CrossRef]
18. Almajid, M.M.; Abu-Al-Saud, M.O. Prediction of porous media fluid flow using physics informed neural networks. *J. Pet. Sci. Eng.* **2022**, *208*, 109205. [CrossRef]
19. Depina, I.; Jain, S.; Mar Valsson, S.; Gotovac, H. Application of physics-informed neural networks to inverse problems in unsaturated groundwater flow. *Georisk Assess. Manag. Risk Eng. Syst. Geohazards* **2021**, *16*, 21–36. [CrossRef]
20. Bandai, T.; Ghezzehei, T.A. Physics-Informed Neural Networks with Monotonicity Constraints for Richardson-Richards Equation: Estimation of Constitutive Relationships and Soil Water Flux Density from Volumetric Water Content Measurements. *Water Resour. Res.* **2021**, *57*, e2020WR027642. [CrossRef]
21. Zhang, Z. A physics-informed deep convolutional neural network for simulating and predicting transient Darcy flows in heterogeneous reservoirs without labeled data. *J. Pet. Sci. Eng.* **2022**, *211*, 110179. [CrossRef]
22. Bekele, Y.W. Physics-informed deep learning for one-dimensional consolidation. *J. Rock Mech. Geotech. Eng.* **2021**, *13*, 420–430. [CrossRef]
23. Waheed, U.b.; Haghighat, E.; Alkhalifah, T.; Song, C.; Hao, Q. PINNeik: Eikonal solution using physics-informed neural networks. *Comput. Geosci.* **2021**, *155*, 104833. [CrossRef]
24. Cuomo, S.; Di Cola, V.S.; Giampaolo, F.; Rozza, G.; Raissi, M.; Piccialli, F. Scientific Machine Learning Through Physics–Informed Neural Networks: Where we are and What's Next. *J. Sci. Comput.* **2022**, *92*, 88. [CrossRef]
25. Haghighat, E.; Raissi, M.; Moure, A.; Gomez, H.; Juanes, R. A physics-informed deep learning framework for inversion and surrogate modeling in solid mechanics. *Comput. Methods Appl. Mech. Eng.* **2021**, *379*, 113741. [CrossRef]
26. Rendulic, L. Porenziffer und Porenwasserdruck in Tonen. *Bauingenieur* **1936**, *17*, 559–564.
27. Garnelo, M.; Shanahan, M. Reconciling deep learning with symbolic artificial intelligence: Representing objects and relations. *Curr. Opin. Behav. Sci.* **2019**, *29*, 17–23. [CrossRef]